Journal of Power Sources 185 (2008) 577–583

Contents lists available at ScienceDirect

Journal of Power Sources

journal homepage: www.elsevier.com/locate/jpowsour

Controlled synthesis and photocatalytic investigation of different-shaped one-dimensional titanic acid nanomaterials

Qiuye Li[a,b,c], Gongxuan Lu[a,*]

[a] State Key Laboratory for Oxo Synthesis and Selective Oxidation, Lanzhou Institute of Chemical Physics, Chinese Academy of Sciences, Lanzhou 730000, China
[b] The Graduate School of the Chinese Academy of Sciences, Chinese Academy of Sciences, Beijing 10080, China
[c] Key Laboratory of Special Functional Materials, Henan University, KaiFeng 475001, China

ARTICLE INFO

Article history:
Received 11 June 2008
Accepted 16 June 2008
Available online 25 June 2008

Keywords:
Dye sensitization
Eosin Y
One-dimensional TiO_2-based nanomaterials
Photocatalytic hydrogen generation
Visible light irradiation

ABSTRACT

Different-shaped one-dimensional (1D) titanic acid nanomaterials (TANs) were prepared by hydrothermal synthesis. By changing the reaction temperature (120, 170 and 200 °C), three kinds of 1D TAN, short-nanotubes (SNT), long-nanotubes (LNT), and nanorods (NR), were obtained. The obtained TANs were characterized by transmission electron microscopy (TEM), high-resolution transmission electron microscopy (HRTEM), powder X-ray diffraction (XRD), and solid-stated diffuse reflectance UV–vis spectra (UV–vis DRS) techniques. Based on these 1D TAN, Eosin Y-sensitized Pt-loaded TAN were prepared by the in situ impregnation and photo-reduction method. Their photocatalytic activity for hydrogen generation was evaluated in triethanolamine (TEOA) aqueous solution under visible light irradiation ($\lambda \geq 420$ nm). The results indicated that the morphology difference led to a significant variation of photocatalytic performance for hydrogen generation, with the activity order as follows: Eosin Y-sensitized Pt-loaded LNT > Eosin Y-sensitized Pt-loaded NR > Eosin Y-sensitized Pt-loaded SNT. The experimental conditions for photocatalytic hydrogen generation such as Pt loading content, the mass ratio of Eosin Y to TAN, and so on, were optimized. As a result, the highest apparent quantum yields of hydrogen generation for Eosin Y-sensitized Pt-loaded SNT, LNT, and NR were 6.65, 17.36, and 15.04%, respectively. The stability of these photocatalysts and the reaction mechanism of the photocatalytic hydrogen generation are also discussed in detail.

1. Introduction

Nanosized materials with special properties have already led to a breakthrough in various fields of science and technology. Nanosized TiO_2 is widely used in photocatalysis, solar cells and nanophotonic devices, owing to its high efficiency, good chemical stability, non-toxicity and low cost. Since the discovery of carbon nanotubes [1], one-dimensional (1D) nanostructured materials (nanotubes, nanowires, nanorods, and nanobelts) have been subject to intensive study due to their peculiar geometries, novel physicochemical properties, and potential applications in numerous areas such as nanoscale electronics and photonics. Consequently, TiO_2-based 1D nanomaterials have already attracted extensive interest in the fields of nano-organization, photo-electrochemical cells, photocatalysis, and so on. Many methods have been used to fabricate 1D TiO_2-based nanomaterials, including sol-gel [2], templates [3], electrochemical anodic oxidation [4] and hydrothermal synthesis [5–7]. Among these methods, hydrothermal synthesis is easy to manipulate and is widely used [8–10]. Kasuga et al. was the first to prepare TiO_2 nanotubes by hydrothermal synthesis [5]. Following this Yang et al. analyzed their composition and structure systematically, and verified their chemical composition as $H_2Ti_2O_4(OH)_2$ [6]. Zhang et al. investigated the effect of annealing temperature on their physicochemical properties and applied them to the photocatalytic oxidation of propylene [11]. Yu et al. fabricated a series of TiO_2 nanorods, nanotubes [12], nanowires [13], nanofibers [14], hollow microspheres [15] and mesoporous powders [16] by hydrothermal synthesis [5] and found that their photocatalytic activity was much greater than that of P25, attributing this to their larger specific surface areas and higher pore volumes.

Although 1D TiO_2-based nanomaterials have many special merits, their large energy band gap (~3 eV) remains the biggest obstacle to expansion of their usage [17,18]. Dye sensitization is an efficient way to expand the absorption range of a semiconductor, and has been widely used in solar cell [19] and visible-light-induced photocatalysis [20–22]. Recently, we reported that dye-sensitized Ti-MCM-41 zeolite and multi-walled carbon nanotubes (MWCNT) have an enhanced photocatalytic activity for hydrogen generation [20,21]. We also prepared dye-sensitized nanotube sodium titanate

* Corresponding author. Tel.: +86 931 4968178; fax: +86 931 4968178.
E-mail address: gxlu@lzb.ac.cn (G. Lu).

0378-7753/$ – see front matter © 2008 Elsevier B.V. All rights reserved.
doi:10.1016/j.jpowsour.2008.06.043

(NTS), and compared its photocatalytic activity with dye-sensitized TiO_2 [22].

In this work we prepared three 1D TAN, with different structures, by hydrothermal synthesis, and investigated the effect of morphology on the photocatalytic activity of hydrogen generation on Eosin Y-sensitized Pt-loaded 1D TAN under visible light irradiation. The experimental conditions for photocatalytic hydrogen production were optimized, and the reaction mechanism was also elucidated in detail.

2. Experimental

2.1. Preparation of 1D titanic acid nanomaterials

1D TANs were prepared by hydrothermal synthesis using a method similar to that described by Kasuga et al. [5] and Yang et al. [6]. Typically, 1 g of TiO_2 (P25, Degussa AG, Germany) was added to 60 mL of 10 M NaOH solution, and dispersed ultrasonically for 10 min, then transferred into a Teflon-lined autoclave to react for 24 h at different temperatures (120, 170, 200 °C). Afterwards, the precipitate was filtered and washed with distilled water to pH 7, and then the pH value adjusted to 1 using 0.1 M HCl aqueous solution. The suspension was stirred for 5 h, and then washed with distilled water until no Cl^- was detectable. The washed samples were dried in an oven at 60 °C for 24 h.

2.2. Preparation of Eosin Y-sensitized Pt-loaded 1D TAN and evaluation of their photocatalytic activities for hydrogen generation

The photocatalytic reaction was carried out in a 140-mL Pyrex flask, with a flat window (an effective irradiation area of 10 cm^2). A 300-W tungsten halogen lamp, equipped with a 420 nm cut-off filter (Toshiba, SY44.2), was used as the light source. Eosin Y-sensitized Pt-loaded 1D TAN catalysts were prepared using the in situ impregnation and photo-reduction method. Typically, 20 mg of 1D TAN, with the calculated amount of Eosin Y and H_2PtCl_6 aqueous solution, were suspended in TEOA–H_2O mixture (80 mL, 15 vol%) by magnetic stirring. Prior to irradiation, the suspension was dispersed ultrasonically for 1 min, and then Ar gas was bubbled through the reaction mixture to remove oxygen for 40 min. The photocatalytic activity was estimated by measuring the amount of hydrogen production using a gas chromatograph (thermal conductivity detector (TCD), molecular sieve 5A column, Ar as gas carrier). The pH value of the reaction solution was adjusted by addition of hydrochloric acid or sodium hydroxide using a Markson 6200 model pH meter.

2.3. Adsorption curves of Eosin Y on different-shaped 1D TAN

The experimental conditions for adsorption of Eosin Y on different 1D TANs were similar to those of the photocatalytic reaction system. 20 mg of SNT (or LNT or NR), and the calculated amount of Eosin Y were added to 80 mL of TEOA solution, dispersed ultrasonically for 10 min, and stirred for 24 h to saturate. The adsorption amount of Eosin Y was calculated from the absorbance difference between the initial sensitizer solution and the filtered solution of the suspension with 1D TAN added.

2.4. Characterization

TEM and HRTEM images were taken on a JEOL JEM-2010 electron microscope operating at 100 kV. XRD patterns of the photocatalysts were recorded on a Rigakel B/Max-RB diffractometer with a nickel filtered Cu Kα radiation. UV–vis DRS of the samples were recorded with a U-3010 UV–vis spectrometer equipped with an integrating sphere diffuse reflectance accessory, using $BaSO_4$ as a reference.

3. Results and discussion

3.1. Characterization of the three 1D TANs with different shapes

Fig. 1 shows the TEM images of three samples of 1D TANs prepared at different hydrothermal temperatures. As can be seen, when the reaction temperature is controlled at 120 °C, a large quantity of short-nanotubes are formed with a diameter of 10–20 nm and length about 80–150 nm. As the temperature increases, the nanotubes become longer and expand to several micrometers, but their diameters remain approximately unchanged. This indicates that the crystallization improves as the temperature increases, which was also verified by the XRD patterns (Fig. 2). Comparing curves a and b of Fig. 2, we can see that the characteristic peaks of titanate become sharper and stronger as the temperature increases. However, the morphology changes to thick nanorods when the temperature increases to 200 °C, and the crystallization is much better. The lengths of the nanorods are several micrometers and some of nanorods are tied into bundles.

Fig. 2 shows the XRD patterns of the three shapes of 1D TAN. Curves a and b are similar, but different to curve c, indicating that the synthesis temperature may induce a significant change in the phase structure of these titanate compounds. The diffraction peak at about $2\theta = 10^\circ$ is assigned to the (2 0 0) crystal face of layered titanate, which is its characteristic peak. Comparing a and b, the reflection peak at $2\theta = 10^\circ$ of curve c shifts to a higher angle, and the intensity becomes greater and the peak sharper, indicating that the interlayer spacing decreases [23]. There is a broad peak at about $2\theta = 24.5^\circ$, which can be assigned to hydrogen titanate compounds according to standard XRD data. Moreover, there exists a diffraction peak around $2\theta = 48.5^\circ$, which may be ascribed to sodium titanate compounds [23,24]. As we know, sodium titanate is formed first after hydrothermal synthesis, and the sodium ions exchange with protons when they are washed with HCl solution. Therefore, sodium ions may not have been exchanged completely.

Fig. 3 shows the UV–vis DRS of the three forms of 1D TAN. As can be seen, SNT and LNT have higher absorption ability compared with NR, but all of them have the similar band structures. According to the onset wavelength of the three semiconductors (411, 413, 405 nm), their band energies (Eg) are calculated to 3.02, 3.00 and 3.06 eV, respectively. These results indicate that all the semiconductors can only be excited by UV light. Utilizing the visible light of the solar spectrum is attracting extensive attention of many scientists all over the world. Hence, if we want to expand the use of these semiconductors, some modifications must be conducted. Dye sensitization is an efficient and easy way to expand the absorption range of a semiconductor, and has been successfully used in our former work [20–22,25–27].

3.2. Optimization of the photocatalytic reaction conditions for hydrogen generation

The energy bands of all the three forms of 1D TAN are about 3 eV, indicating that they can only be excited by UV light. However, they can work under visible light after being sensitized by Eosin Y. The photocatalytic activity is influenced by many factors, such as the pH value, dye concentration, noble metal loading content, and so on. The effect of pH value on Eosin Y-sensitized photocat-

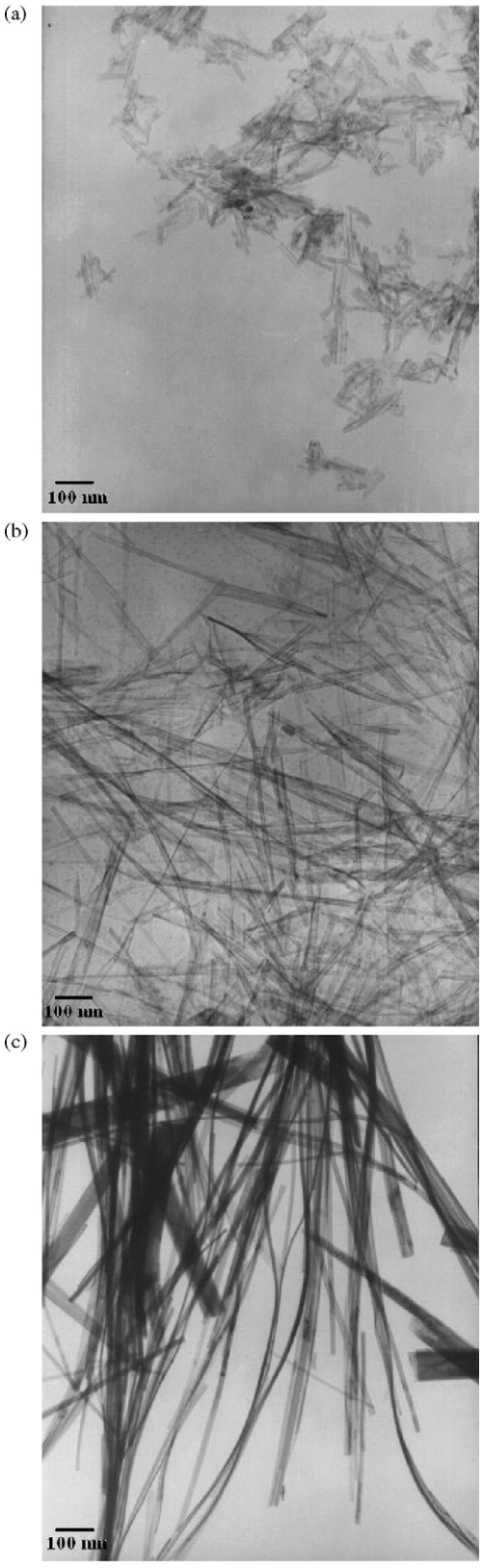

Fig. 1. TEM images of 1D TAN (a) short-nanotube, (b) long-nanotube, and (c) nanorod.

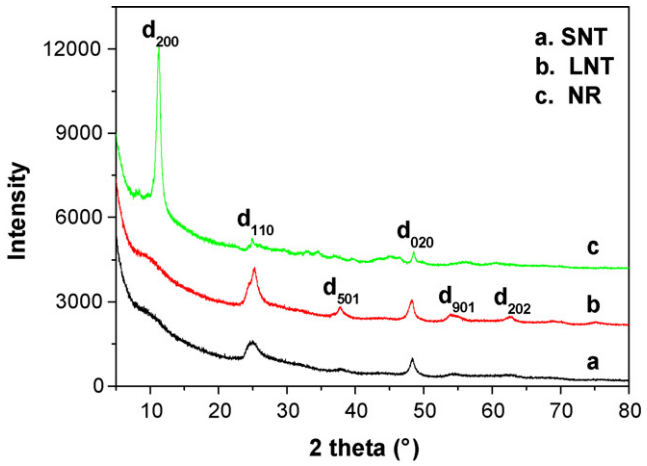

Fig. 2. XRD patterns of the three forms of 1D TAN.

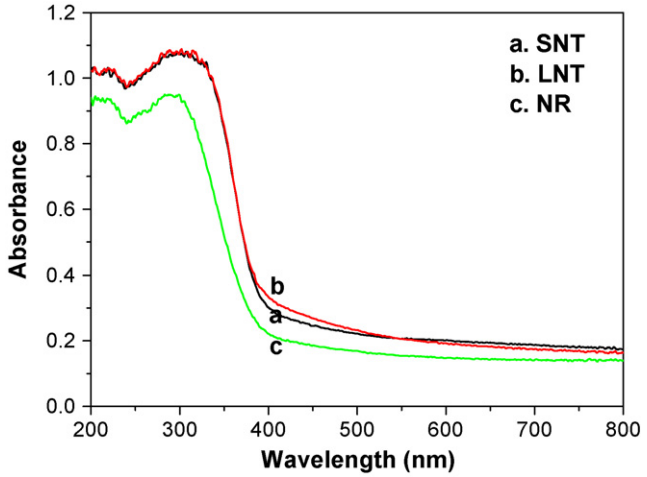

Fig. 3. UV–vis DRS of the three forms of 1D TAN.

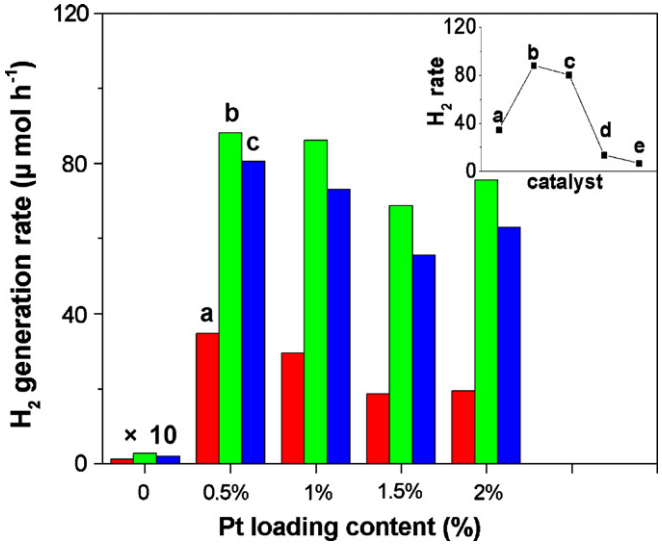

Fig. 4. Effect of the Pt loading content on the hydrogen generation rate. The inset is a comparison of the hydrogen generation rate at 0.5% Pt loading content. (a) Eosin Y-sensitized Pt-loaded SNT, (b) Eosin Y-sensitized Pt-loaded LNT, (c) Eosin Y-sensitized Pt-loaded NR, (d) Eosin Y-sensitized Pt-loaded TiO_2, (e) Eosin Y-sensitized Pt nanoparticles. Reaction condition: $E/T = 1$; pH 7; Ar atmosphere. The symbol "×10" means that the amount of hydrogen is magnified 10 times.

alytic hydrogen generation system has been investigated in our previous work, and the optimum activity was obtained at pH 7 [20–22]. Therefore, the photocatalytic reaction of the three forms of Eosin Y-sensitized 1D TAN is conducted in neutral aqueous solutions.

3.2.1. *Effect of the Pt loading content on the photocatalytic activity for hydrogen generation*

Noble metals, such as Pt, or transition metal oxides are usually loaded on to a catalyst as a co-catalyst in photocatalytic water splitting. Pt is always widely used as it is the most efficient co-catalyst

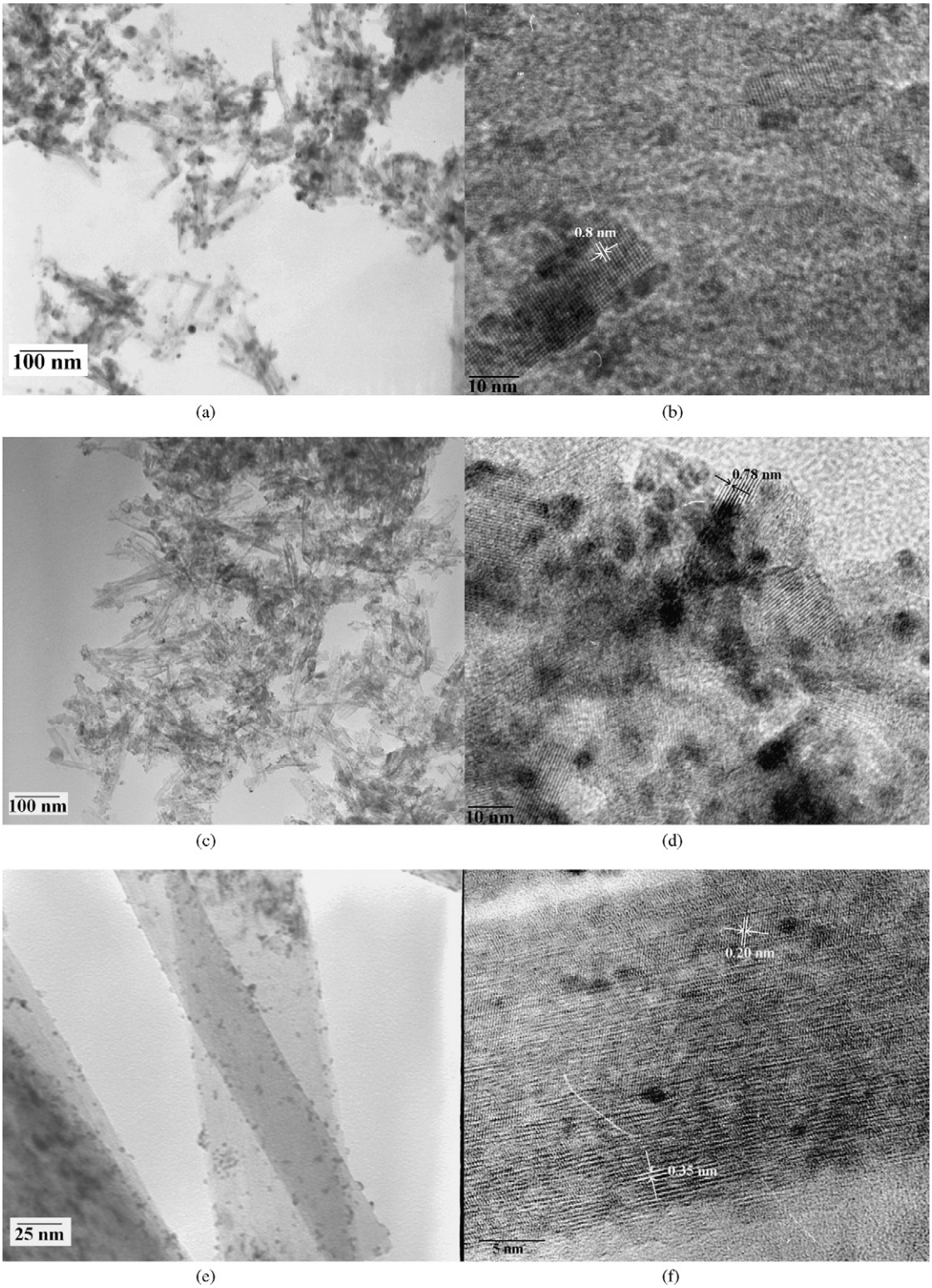

Fig. 5. TEM and HRTEM images of Pt-loaded 1D TAN. The Pt loading content is 0.5%. (a) Pt-loaded SNT, (b) HRTEM of Pt-loaded SNT, (c) Pt-loaded LNT, (d) HRTEM of Pt-loaded LNT, (e) Pt-loaded NR, (f) HRTEM of Pt-loaded NR.

due to its high work function and low Fermi energy. In addition, Pt is a well-known active site for hydrogen generation [28,29]. The effect of Pt loading content on the photocatalytic activity of Eosin Y-sensitized 1D TAN is illustrated in Fig. 4. As can be seen, the hydrogen generation rates are similar when the Pt loading content is 0.5% and 1%, and then decrease if the content is increased further. When the Pt loading content is high (>1%), there have been two reasons proposed to interpret the decrease of photocatalytic activity. On the one hand, excessive Pt loading will result in the growth and agglomeration of Pt nanoparticles, which will absorb and scatter some incident light [30]. On the other hand, the loaded Pt nanoparticles not only act as separation sites for photogenerated carriers, but also act as recombination sites. The separation and recombination processes compete with each other. With excessive loading of Pt nanoparticles, more electrons aggregate on their surface and the recombination probability increases; as a result, the photocatalytic activity will decrease. However, the H_2 generation rate is very low over the Pt-free samples, indicating that Pt nanoparticles play an important role in the photocatalytic reaction. When the Pt loading content is 0.5%, the hydrogen generation rate is 34.8, 88.1 and 80.5 μmol h^{-1} for Eosin Y-sensitized SNT, LNT and NR, respectively. The inset figure illustrates that the photocatalytic activity of the Eosin Y-sensitized Pt-loaded 1D TAN is much higher than that of Eosin Y-sensitized Pt-loaded TiO_2 and Eosin Y-sensitized Pt nanoparticles. The reasons for this have been discussed in our earlier papers [21,22].

Fig. 5 shows the TEM and HRTEM images of Eosin Y-sensitized Pt-loaded SNT, LNT and NR. As can be seen, Pt nanoparticles are successfully deposited on the surface of 1D TAN; their diameter is about 3–5 nm and the size is relatively uniform. This indicates that the in situ photo-reduction method is a good and efficient way to prepare catalysts loaded with small nanoparticles of noble metals. By observing the HRTEM pictures, we can also see that the interlayer spacing of SNT and LNR is almost same, about 0.8 nm. This is consistent with the data reported by Yang et al. [6]. However, the interlayer spacings of NR are only 0.35 and 0.20 nm. This result has the same characteristic as the XRD result, where the interlayer spacing decreases when temperature is increased from 170 to 200 °C. Comparing Figs. 1 and 5, we find that the lengths of the SNT and LNT become shorter after reaction, while the structure of NR remains integrated and perfect.

3.2.2. *Effect of the concentration of Eosin Y on the photocatalytic activity for hydrogen generation*

The concentration of the dye has a large effect on the photocatalytic activity in dye-sensitized reaction systems, a feature which is related to the reaction mechanism. In our work, Eosin Y molecules are adsorbed on to the surface of the 1D TAN and Pt nanoparticles. Under visible light irradiation, dye molecules absorb visible light and their electrons are excited from the HOMO to the LUMO state. The excited electrons are trapped by 1D TAN, and then transferred to Pt nanoparticles, or are injected into Pt nanoparticles directly, and then participate in the photocatalytic water reduction for hydrogen evolution. The concentration of Eosin Y plays a key role in the number of excited electrons involved, so it is very important to investigate the effect of the concentration of Eosin Y on the photocatalytic activity. The results from catalysts with 0.5% Pt loading content are shown in Fig. 6. The mass ratio of Eosin Y to 1D TAN is denoted as E/T. As can be seen, the activity is enhanced as E/T increases, reaches a peak when $E/T = 5/4$, then decreases. This phenomenon can be explained by the absorption curves of Eosin Y on TAN (Fig. 7). As can be seen, the amount of Eosin Y adsorbed on all three different-shaped TAN increases as E/T increases, and reaches saturation at $E/T = 5/4$ approximately. The highest photocatalytic activity obtained at $E/T = 5/4$ can be interpreted by the following: when E/T is small, the amount of Eosin Y molecules adsorbed increases with the increase of E/T, so the number of electrons used for reduction of water to hydrogen generation increases. When the adsorption approaches saturation, it is disadvantageous to the photocatalytic reaction if E/T increases further. That is because the free dye molecules in solution cannot participate in the electron transfer. By contrast, they absorb a part of incident light leading to a loss of a fraction of light for water reduction. Thus, the photocatalytic activity declines correspondingly.

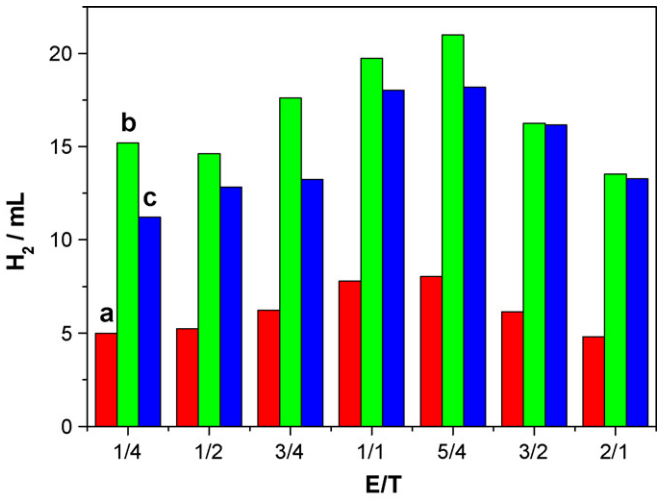

Fig. 6. Effect of the mass ratio of Eosin Y and 1D TAN (E/T) on the photocatalytic activity of hydrogen generation. (a) Eosin Y-sensitized Pt-loaded SNT, (b) Eosin Y-sensitized Pt-loaded LNT, (c) Eosin Y-sensitized Pt-loaded NR. Reaction condition: 0.5% Pt loading content; pH 7; Ar atmosphere.

3.3. *Effect of the morphology of 1D TAN on the photocatalytic performance*

From Figs. 4 and 6, we can see that the photocatalytic activity of the three forms of Eosin Y-sensitized Pt-loaded TAN is different under the same experimental conditions, in the following order: Eosin Y-sensitized Pt-loaded LNT (b) > Eosin Y-sensitized Pt-loaded NR (c) > Eosin Y-sensitized Pt-loaded SNT (a). This phenomenon can be explained as follows.

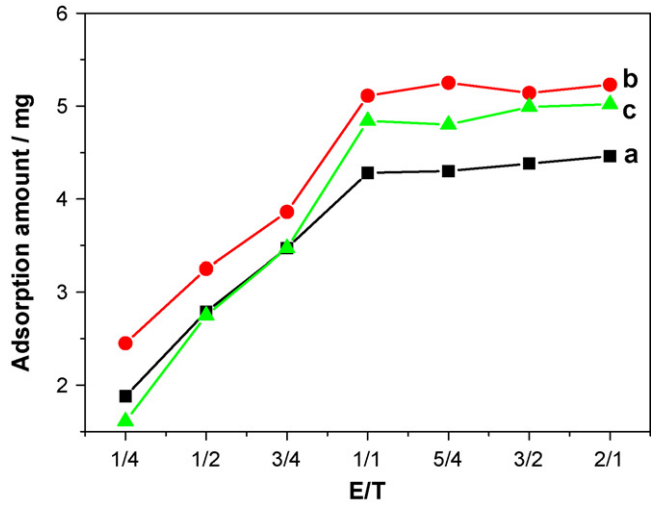

Fig. 7. The adsorption curves of Eosin Y on different 1D TANs in TEOA solution. (a) Eosin Y/SNT; (b) Eosin Y/LNT; (c) Eosin Y/NR.

The first factor is the effect of the degree of adsorption of dye molecules on the photocatalytic activity. From Fig. 7, we can see that the adsorption of Eosin Y on the three forms of 1D TAN follows the order LNT > NR > SNT. The degree of adsorption is consistent with that of photocatalytic activity. According to the reaction mechanism of the dye-sensitized photocatalyst system, we know that more dye adsorption will result in higher photocatalytic activity.

The second factor is the effect of the morphology on the photocatalytic activity. Catalysts a and b are nanotubes and the interspaces are hollow, so there must have been some dye inside the nanotubes that cannot be excited under irradiation. However, Eosin Y in the NR system can be excited completely.

The last factor is the effect of the defect sites on the photocatalytic activity. As can be seen from the HRTEM images of the three catalysts (Fig. 5), the crystallization of Eosin Y-sensitized Pt-loaded SNT and LNT is weak and they have more defect sites, while the crystallization of Eosin Y-sensitized Pt-loaded NR is perfect and integrated. It is well known that defect sites are the combination centers of photogenerated electron and hole pairs. If one catalyst has more defect sites, the combination probability of the photogenerated carriers will increase, and the photocatalytic activity will be reduced [31,32].

Therefore, based on the three factors described above, Eosin Y-sensitized Pt-loaded LNT exhibits the highest activity for photocatalytic hydrogen generation; Eosin Y-sensitized Pt-loaded NR is next, and Eosin Y-sensitized Pt-loaded SNT is the last.

3.4. Stability of the three forms of Eosin Y-sensitized Pt-loaded 1D TAN photocatalysts

Stability is one of the important properties of a catalyst. Fig. 8 shows the stability of photocatalytic H_2 production on Eosin Y-sensitized Pt (0.5 wt%)-loaded TAN (E/T = 5/4) in TEOA solution at pH 7. As can be seen, the hydrogen generation rates in the first run are 1.80, 4.69, 4.06 mmol h^{-1} g^{-1} for Eosin Y-sensitized Pt-loaded SNT (a), LNT (b) and NR (c), respectively. The apparent quantum yields of hydrogen generation can be calculated according to the equation in reference [20], and are 6.65%, 17.36%, and 15.04%, respectively. The yield of Eosin Y-sensitized Pt-loaded LNT is much higher than that of our earlier reported value of 14.97% [22]. Moreover, we can also see that the rate reaches its maximum in the third run, and then declines gradually in consecutive runs for catalysts a and b. However, the rate with catalyst c only declines slightly in all six runs. For all three photocatalysts, the modest decrease of hydrogen generation rate is probably caused by the consumption of electron donor (TEOA) and the partial decomposition of Eosin Y. Another reason for the decrease of the generation rate with catalysts a and b is probably due to the collapse of the structures of the SNT and LNT. From Fig. 1, we find that the nanotubes structures of the LNT and SNT nanotubes are complete, but are destroyed after reacting for a long time, and more defect sites form after reaction (in Fig. 5). However, the structure of NR remains undamaged after reaction. When another portion of Eosin Y and TEOA were added to the system after reaction, the photocatalytic activity recovered for Eosin Y-sensitized Pt-loaded NR, but catalysts a and b did not because their structures had been partly destroyed.

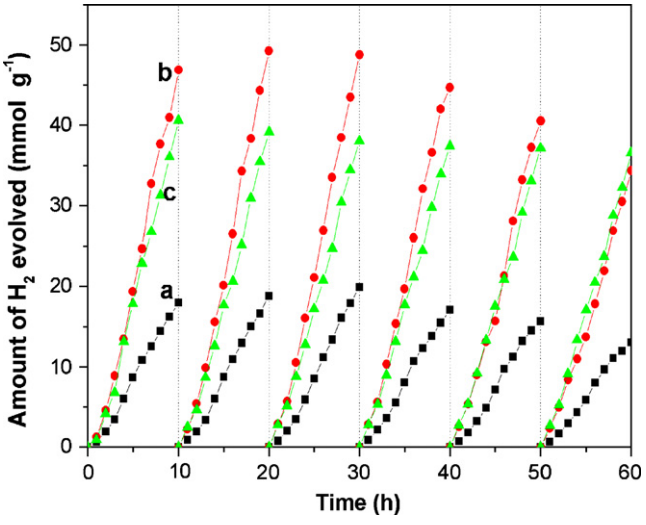

Fig. 8. Stability of the three kinds of Eosin Y-sensitized Pt-loaded TAN photocatalysts. (a) Eosin Y-sensitized Pt-loaded SNT, (b) Eosin Y-sensitized Pt-loaded LNT, (c) Eosin Y-sensitized Pt-loaded NR. Reaction condition: 0.5% Pt loading content, E/T = 5/4, pH 7, Ar atmosphere.

4. Conclusion

Three forms of 1D titanic acid nanomaterials (SNT, LNT, and NR) were prepared by hydrothermal synthesis at 120, 170 and 200 °C, respectively. HRTEM images showed that the interlayer spacing of the SNT and LNT was about 0.8 nm, while that of the NR was only 0.35 and 0.20 nm. UV–vis DRS results showed that their energy gaps (Eg) were about 3 eV, indicating that they could be excited only by UV light. Based on these nanomaterials, three kinds of Eosin Y-sensitized Pt-loaded 1D TAN were prepared by the in situ impregnation and photo-reduction method, and their photocatalytic performance was investigated under visible light irradiation ($\lambda \geq 420$ nm). The morphologies had a large effect on the photocatalytic activity for hydrogen generation, in the following order: Eosin Y-sensitized Pt-loaded LNT > Eosin Y-sensitized Pt-loaded NR > Eosin Y-sensitized Pt-loaded SNT.

The optimized reaction conditions for photocatalytic hydrogen generation were investigated, with Pt loading content at 0.5% and the mass ratio E/T = 5/4. The highest apparent quantum yield of hydrogen generation over Eosin Y-sensitized Pt-loaded SNT, LNT and NR are 6.65%, 17.36%, and 15.04%, respectively. Among these, the Eosin Y-sensitized Pt-loaded LNT exhibited the highest photocatalytic activity, due to its greater adsorption of dye molecules, while Eosin Y-sensitized Pt-loaded NR exhibited the greatest stability because of its perfect and integrated crystallization structure.

Acknowledgements

Financial support from the Natural National Science Foundation of China (No. 90210027) and the National Basic Research Program of China (Nos. 2003CB214500 and 2007CB613305) is gratefully acknowledged.

References

[1] S. Lijima, Nature 354 (1991) 56–58.
[2] Q. Zeng, Z. Zhang, Z. Ding, Y. Wang, Y. Sheng, Scripta Mater. 57 (2007) 897–900.
[3] J.H. Jung, H. Kobayashi, K.J.C. Van Bommel, S. Shinkai, T. Shimizu, Chem. Mater. 14 (2002) 1445–1447.
[4] A. Ghicov, H. Tsuchiya, J.M. Macak, P. Schmuki, Electrochem. Commun. 7 (2005) 505–509.
[5] T. Kasuga, M. Hiramatsu, A. Hoson, T. Sekino, K. Niihara, Langmuir 14 (1998) 3160–3163.
[6] J. Yang, Z. Jin, X. Wang, W. Li, J. Zhang, S. Zhang, X. Guo, Z. Zhang, Dalton Trans. (2003) 3898–3901.
[7] S. Zhang, W. Li, Z. Jin, J. Yang, J. Zhang, Z. Du, Z. Zhang, J. Solid State Chem. 11 (2004) 1365–1371.
[8] J. Liu, G. Chen, Z. Li, Z. Zhang, Int. J. Hydrogen Energy 32 (2007) 2269–2272.
[9] Y. Ryu, M. Lee, E. Jeong, H. Kim, W. Jung, S. Baek, G. Lee, S. Park, S. Hong, Catal. Today 124 (2007) 88–93.
[10] H. Fu, L. Zhang, W. Yao, Y. Zhu, Appl. Catal. B: Environ. 66 (2006) 100–110.
[11] M. Zhang, Z. Jin, J. Zhang, X. Guo, J. Yang, W. Li, X. Wang, Z. Zhang, J. Mol. Catal. A: Chem. 217 (2004) 203–210.

[12] H. Yu, J. Yu, B. Cheng, J. Lin, J. Hazard. Mater. 147 (2007) 581–587.
[13] H. Yu, J. Yu, B. Cheng, Chemosphere 66 (2007) 2050–2057.
[14] J. Yu, H. Yu, B. Cheng, X. Zhao, Q. Zhang, J. Photochem. Photobiol. A: Chem. 182 (2006) 121–127.
[15] J. Yu, S. Liu, H. Yu, J. Catal. 249 (2007) 59–66.
[16] J. Yu, Y. Su, B. Cheng, M. Zhou, J. Mol. Catal. A: Chem. 258 (2006) 104–112.
[17] Q. Li, J. Zhang, Z. Jin, D. Yang, X. Wang, J. Yang, Z. Zhang, Electrochem. Commun. 8 (2006) 741–746.
[18] Q. Li, X. Wang, Z. Jin, D. Yang, S. Zhang, X. Guo, J. Yang, Z. Zhang, J. Nanopart. Res. 9 (2007) 951–957.
[19] B.O. Regan, M. Grätzel, Nature 353 (1991) 737–739.
[20] Q. Li, Z. Jin, Z. Peng, Y. Li, S. Li, G. Lu, J. Phys. Chem. C 111 (2007) 8237–8241.
[21] Q. Li, L. Chen, G. Lu, J. Phys. Chem. C 111 (2007) 11494–11499.
[22] Q. Li, G. Lu, J. Mol. Catal. A: Chem. 266 (2007) 75–79.
[23] R. Yoshida, Y. Suzuki, S. Yoshikawa, Mater. Chem. Phys. 91 (2005) 409–416.
[24] L. Weng, S. Song, S. Hodgson, A. Baker, J. Yu, J. Eur. Ceram. Soc. 26 (2006) 1405–1409.
[25] Z. Jin, X. Zhang, Y. Li, S. Li, G. Lu, Catal. Commun. 8 (2007) 1267–1273.
[26] Z. Jin, X. Zhang, G. Lu, S. Li, J. Mol. Catal. A: Chem. 259 (2006) 275–280.
[27] X. Zhang, Z. Jin, Y. Li, S. Li, G. Lu, J. Power Sources 166 (2007) 74–79.
[28] T. Abe, E. Suzuki, K. Nagoshi, K. Miyashita, M. Kaneko, J. Phys. Chem. B 103 (1999) 1119–1123.
[29] W. Shangguan, A. Yoshida, J. Phys. Chem. B 106 (2002) 12227–12230.
[30] H. Yi, T. Peng, D. Ke, A. Ke, L. Zan, C. Yan, Int. J. Hydrogen Energy 33 (2008) 672–678.
[31] H. Kato, A. Kudo, J. Phys. Chem. B 105 (2001) 4285–4292.
[32] K. Maeda, K. Domen, J. Phys. Chem. C 111 (2007) 7851–7861.